

Atomic structure dependence of nonsequential double ionization of He, Ne and Ar in strong laser pulses

V.L. Bastos de Jesus, B. Feuerstein, K. Zrost, D. Fischer, A. Rudenko, F. Afaneh, C.D.

Schröter, R. Moshhammer, and J. Ullrich

Max-Planck-Institut für Kernphysik, D-69029 Heidelberg, Germany

The ion momentum spectra for nonsequential double ionization of rare gases (He, Ne, and Ar) in 23 fs 795-nm laser pulses were measured in the intensity range between 0.075 and 1.25 PW/cm². Confusing differences in the shape of so far published momentum distributions between the different targets are consistently explained within a recollision scenario: Excitation during recollision plus subsequent field ionization, not implemented in most theoretical approaches, is provided evidence to play a decisive role for He and Ar nonsequential double ionization whereas it plays only a minor role for Ne.

32.80.Rm, 31.90.+s, 32.80.Fb

Many-electron dynamics in intense laser fields has been the subject of a large number of theoretical and experimental investigations. In particular, strong field double ionization is a fundamental process and, at the same time, one of the most challenging problems in atomic and optical physics, theoretically as well as experimentally. Whereas single ionization is well understood within the "single active electron" (SAE) model, the

observed yields of double ionization in linearly polarized laser pulses exceed those predicted by the SAE model assuming a sequence of individual single ionization events by many orders of magnitude. Although the underlying mechanism of this nonsequential (NS) double ionization remained unclear over many years, it was agreed that the NS double ionization has to incorporate the correlated two-electron dynamics in intense laser fields (for reviews see ^{1 2}).

Experiments using circularly polarized light as well as recent results exploiting advanced experimental imaging techniques ^{3 4} in agreement with most quantum ^{5 6 7 8 9} as well as classical calculations ^{10 11} provided widely accepted evidence that the so-called rescattering or recollision scenario ¹² is the dominating mechanism for NS double ionization. Here, the first (tunnel-)ionized electron is driven back by the oscillating laser field to its parent ion causing the ionization of a second electron in an (e,2e)-like process. It was shown that the kinematics of this dynamical process is the only one that can explain the double-hump structure of ion momentum distributions along the laser polarization direction ¹³, clearly observed exclusively for Ne²⁺ and Ne³⁺ ions in the NS intensity regime ⁴. However, summarizing the results of published experimental data as well as theoretical predictions for NS double ionization of He, Ne and Ar atoms, one finds a quite confusing situation indicating that the underlying mechanisms are by far not understood.

Singly differential momentum spectra for He²⁺ ions have been measured so far in the intensity range between 0.29 and 0.66 PW/cm². Here, indications of a double-hump structure have only been observed at the highest intensity. Compared to Ne this characteristic feature is much less pronounced and hardly visible at all. In contrast, as

summarized in Fig. 9 of ² most of the theoretical models predict a very clear double-hump shape with a deep minimum at zero momentum not consistent with the experiment. Moreover, and even more surprising the apparently most complete approach, numerical solution of the time-dependent Schrödinger equation for two correlated electrons in a one-dimensional model ⁷ just predicts the opposite behavior, a single maximum at zero momentum, which also does not agree with the experimental findings! Recent calculations by van der Hart revealed ¹⁴ that excitation of He⁺ during recollision followed by subsequent field ionization of the excited electron contributes decisively to double ionization. This mechanism is not considered by anyone of the theoretical models, which actually predict the double-hump behavior. Some of them even correctly reproduce the total rates for multiple ionization without taking this mechanism into account. Finally, a systematic study on the intensity dependence of the ion momentum spectra for Ar²⁺ did not reveal a double-hump structure at all for any intensity ¹⁵! Such a behavior for Ar was recently explained by the recollision-excitation mechanism mentioned above via inspecting correlated electron spectra where the momenta of both emitted electrons are measured in coincidence ¹⁶. In contrast to Ne ¹⁷, the majority of the correlated events violate the kinematical constraints set by conservation of energy and momentum in the recollision-ionization scenario ¹⁶, whereas these data were found to be consistent with the kinematics of recollision-excitation with subsequent field ionization. Due to its sequential nature, this mechanism leads to small drift momenta of one of the electrons, and, thus fills the valley in the ion momentum distribution as observed for He ³ and Ar ^{15 16}.

Consequently, inspecting all available data, severe questions arise, whether the atomic structure can influence the dynamics of NS double ionization, whether such a

potential structure dependence can explain the experimental results for different targets and what really is then the dominant NS double ionization mechanism for the various atomic species. These questions become even more pressing since it is frequently doubted that at such high intensities the atomic structure plays any role at all.

In order to clarify this situation we present a first comprehensive experimental study on the ion momentum distributions of He^{2+} , Ne^{2+} , and Ar^{2+} ions using a novel method for the *in situ* calibration of the intensity in the range between 0.075 and 1.25 PW/cm^2 . Based on a consistent model calculation for the relative contributions of direct (e,2e) ionization and excitation during recollision followed by subsequent field ionization we demonstrate a strong target structure dependence of NS double ionization as well a decisive importance of recollision-excitation: Indeed, we provide convincing evidence that for He and Ar this is the dominant NS ionization mechanism over a wide intensity range. Atomic units are used in the following except indicated otherwise.

For our experiment, we use a Kerr-lens mode locked Ti:sapphire laser at 795 nm wavelength amplified to pulse energies up to 350 μJ at 3 kHz repetition rate. The width of the amplified pulses is 23 fs. After compensation of the astigmatism by means of a spherical mirror telescope the laser beam is focused by a spherical on-axis mirror ($f=100$ mm) to a spot size of 6.5(8) μm on a supersonic gas jet target in an ultra-high vacuum chamber (8×10^{-10} mbar). The focus diameter has been determined from measured optical parameters of the laser beam. Vector momenta of recoil ions emerging from the source volume are recorded using a *reaction microscope* which has been described in detail before¹⁸. The polarization direction of the laser is parallel to the time-of-flight axis of the spectrometer. Along this axis (which is perpendicular to the jet axis) an ion

momentum resolution of 0.1 a.u. is achieved due to collimation of the gas jet. In addition to the conventional method, we determined the laser intensity *in situ* by simultaneously measuring the electron kinetic energy spectra along the laser polarization axis for single ionization. Figure 1 shows such a longitudinal (i.e. parallel to the laser polarization direction) kinetic energy spectrum (log. scale) of the electron for single ionization of Ne along with a Gaussian according to the tunneling theory¹⁹ fitted to the distribution in the region of direct electrons. Since the width of the electron spectrum sensitively depends on the intensity, the fit yields an indirect, online and accurate determination of $I = 0.40(5)$ PW/cm² for the spectrum in Fig. 1. Moreover, as it is well-known, the spectrum shows a distinct change in slope occurring close to the kinetic energy of $2U_p$ (ponderomotive potential $U_p = I/4\omega^2$) indicating the transition from direct and rescattered electrons dominating electron production. At higher energies a *plateau* of rescattered electrons extends up to $\sim 10U_p$ ²⁰. The intensity derived from the fit results in a focus diameter of $5.5(5)$ μm , which agrees well with the value given above. We estimate the accuracy of this method for absolute intensity calibration to be better than 15 %. The relative intensities are derived from the pulse energies measured with < 5 % accuracy, which is *in* at the same time *in* the stability of the laser.

Figure 2 summarizes the measured longitudinal ion momentum spectra for He²⁺, Ne²⁺, and Ar²⁺. We compare the three species at intensities corresponding to the same maximum recollision energy in units of the ionization potential I_p of the singly charged ion $3.17U_p/I_p$. Whereas the shape of the spectra for Ne only shows a weak intensity dependence with a clear double-hump structure everywhere, a distinct transition from a single maximum to a broad structure is observed for Ar and He. At the highest intensity

(1.25 PW/cm²) for He we find for the first time a pronounced minimum at zero momentum at all. For Ar such a behavior cannot be observed at all presumably since the regime of sequential double ionization is already reached at 0.7 PW/cm². The shaded areas indicate the kinematically favored regions based on the recollision (e,2e) model (see Eq. (9) from ¹³). Obviously, for He and Ar another mechanism besides (e,2e) \tilde{n} most likely a sequential excitation tunneling process \tilde{n} plays a crucial role in the doubly charged ion formation.

In order to calculate the relative contributions of direct ionization and excitation tunneling, we use the following semiclassical model within the recollision scenario. In a first step one electron is field-ionized via tunneling at a phase ωt_0 of the oscillating, linearly polarized electric field $F(t) = F_0 \sin(\omega t)$. Depending on the initial phase the electron may be driven back to its parent ion at a phase ωt_1 with a classical recollision energy $E_{rec} = 0.5 F_0^2 \omega^2 [\cos(\omega t_0) \tilde{n} \cos(\omega t_1)]^2$. Here, in a second step electron impact ionization or excitation takes place. In the first case, the second electron is directly ionized in an (e,2e) process, whereas the excitation is followed by subsequent tunneling of the excited electron. In the intensity range considered here this tunneling occurs with almost 100% probability. Thus, for the calculation of the relative contribution of these two mechanisms we only need to calculate the ratio of the effective (phase averaged) yields $Y_{ion,exc}$ for ionization and excitation

$$R = \frac{Y_{ion}}{Y_{exc}}, \quad Y_{ion,exc} = \int_{\pi/2}^{\pi} W_{ADK}(t_0) \sigma_{ion,exc}(E_{rec}(t_0)) d(\omega t_0). \quad (1)$$

Here, $W(\omega t_0)$ is the Ammosov-Delone-Krainov (ADK)¹⁹ static-field tunneling rate. The electron impact cross sections $\sigma_{ion,exc}$ are derived using general, simplified (field-free) expressions. In the case of ionization we use the following formula²¹

$$\sigma_{ion}(E_{rec}) = \sum_{\ell k} C_{\ell} \left(\frac{0.5}{I_p^{+(k)}} \right)^{2-\delta_{\ell}} \xi_{\ell} b_k \frac{\ln \left[1 + (E_{rec} - \tilde{I}_p^{+(k)}) / I_p^{+(k)} \right]}{E_{rec} / I_p^{+(k)}}. \quad (2)$$

The coefficients C_{ℓ} , δ_{ℓ} can be found in²¹. ξ_{ℓ} is the number of equivalent electrons in the initial subshell ℓ and b_k the branching ratio for ionization into a specific term k of the final state. For Ne^+ (Ar^+) we included ionization from the $2p$ ($3p$) and $2s$ ($3s$) subshells. In order to take into account the effect of barrier suppression due to a finite field at the recollision time t_1 we introduce the suppressed ionization potential of the ion²²

$$\tilde{I}_p^+ = I_p^+ - 2\sqrt{2F(t_1)}.$$

The $1s \rightarrow 2\ell$ excitation cross sections for He^+ are taken from a convergent close coupling calculation²³. We extrapolate the cross sections for higher-lying He^+ levels by scaling with known transition strengths²⁴. Since comprehensive data on excitation cross section for Ne^+ and Ar^+ are not available, we use the Van Regemorter formula²⁵ for transitions $i \rightarrow k$

$$\sigma_{exc}^{(ik)}(x) = \frac{2\pi^2 f_{ik} G(x)}{\sqrt{3} E_{ik}^2 x}, \quad x = E_{rec} / E_{ik}, \quad (3a)$$

$$\sigma_{exc}(x) = \sum_{ik} \sigma_{exc}^{(ik)}(x), \quad (3b)$$

with the Gaunt factor $G(x) = 0.349 \ln x + 0.0988 + 0.455x^{\tilde{n}1}$ ²³, the excitation energy E_{ik} , and the absorption oscillator strength f_{ik} (values from²⁴). Figure 3 shows the total cross

sections for He^+ , Ne^+ and Ar^+ as function of the electron impact energy in units of I_p . As expected from the atomic structure (3p-3d transitions) excitation is much stronger in Ar^+ than in Ne^+ . The structure of He^+ is hydrogen-like which results in a reduced ionization cross section compared to excitation since the latter consumes a large amount of the total oscillator strength. The result for the phase-integrated ratio R as a function of the laser intensity is shown in Figure 4. Again, we find a much stronger excitation contribution for He and Ar compared to Ne. This qualitatively explains the different shape of the ion momentum spectra for NS double ionization. For Ar, we can directly compare the calculated ratio $R_{\text{cal}} = 0.37$ at 0.25 PW/cm^2 with the experimental result from ¹⁶ $R_{\text{exp}} = 0.37(6)$ at $0.25(5) \text{ PW/cm}^2$ which is found to be well reproduced by our model.

To conclude, we presented a first comprehensive study on nonsequential double ionization of the noble gases He, Ne and Ar. We used a novel technique for intensity calibration based on the well-established ADK tunneling theory for single ionization electron spectra the result of which agrees well with the intensity derived from the laser beam parameters. A qualitative difference in shape and intensity dependence of the longitudinal momentum spectra of the doubly charged ions is observed for Ne compared to He and Ar, which behave similarly. For the first time a clear double-hump structure in the He^{2+} momentum distribution is observed. We developed a consistent model calculation within the recollision scenario including both (e,2e) and excitation tunneling mechanisms which can \tilde{n} at least qualitatively \tilde{n} explain the substantially different behavior of He/Ar vs. Ne due to differences in the excitation cross sections, caused by the atomic structure. This might be quite surprising considering the fact that we used field-free cross sections; the atomic structure seems to be well preserved even in considerably

perturbed systems. However, at the phases where recollision occurs, the laser field strength is typically small ¹². In order to get more insight into the mechanisms of nonsequential double ionization more kinematically complete studies are planned, in particular for He since this is the only case where an ab initio theoretical description might become available in the future.

This work was supported by the Leibniz-Program of the Deutsche Forschungsgemeinschaft. We are grateful to Tom Kirchner for fruitful discussions.

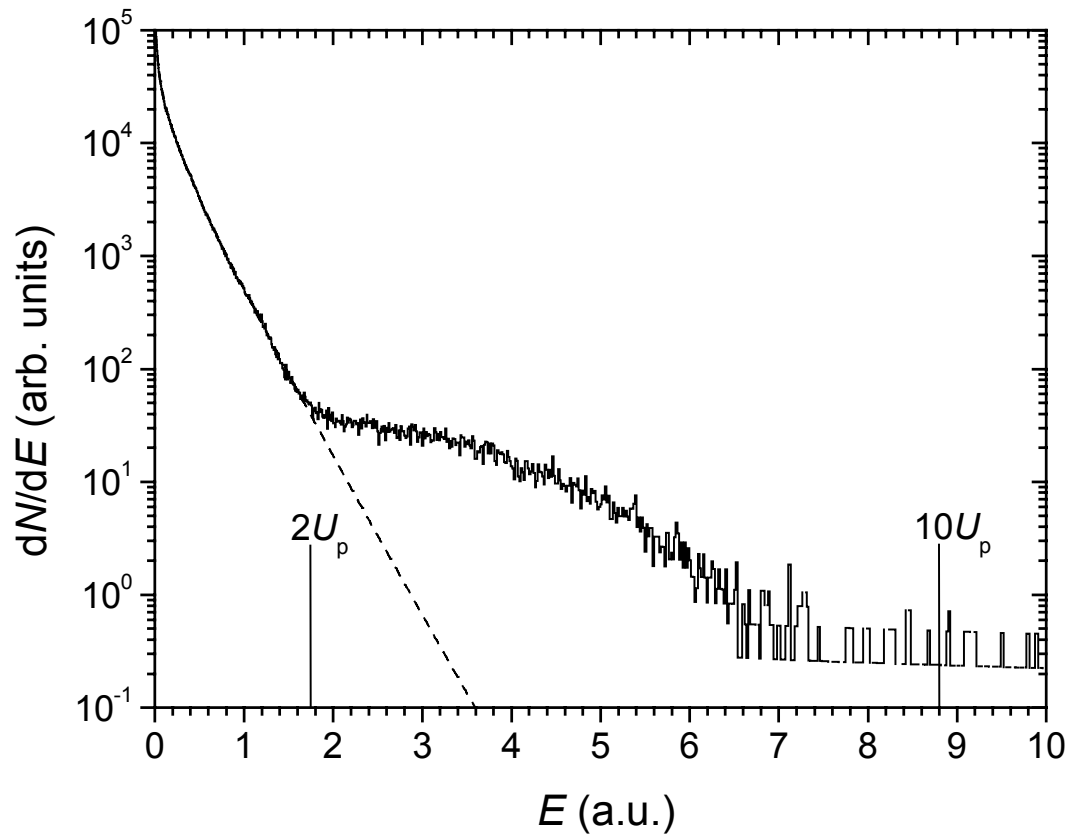


FIG. 1. Longitudinal electron kinetic energy spectrum for single ionization of Ne. The spectrum shows a change in slope close to the kinetic energy of $2U_p$ indicating the transition from direct to rescattered electrons. A Gaussian fit (dashed curve) according to the tunneling theory can, in an indirect way, determine the laser intensity (see text for details).

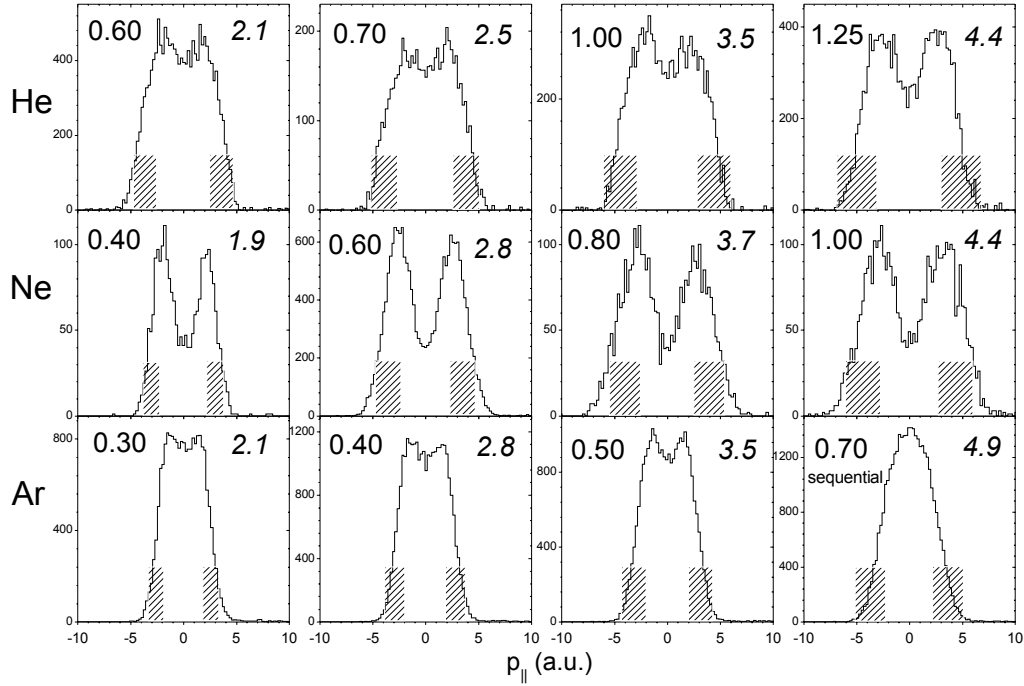


FIG. 2. Ion longitudinal momentum spectra for He^{2+} , Ne^{2+} and Ar^{2+} . The spectra are shown in four columns comparing the three species at intensities (numbers on the left) corresponding to approximately the same maximum recollision energy in units of the ionization potential I_p^+ of the singly charged ion $3.17U_p/I_p^+$ (italic numbers on the right). The shaded areas indicate the kinematically favored regions based on the recollision (e,2e) model (see Eq. (9) from ¹³). Note that at the last spectrum for Ar (0.7 PW/cm²) the sequential regime is already achieved.

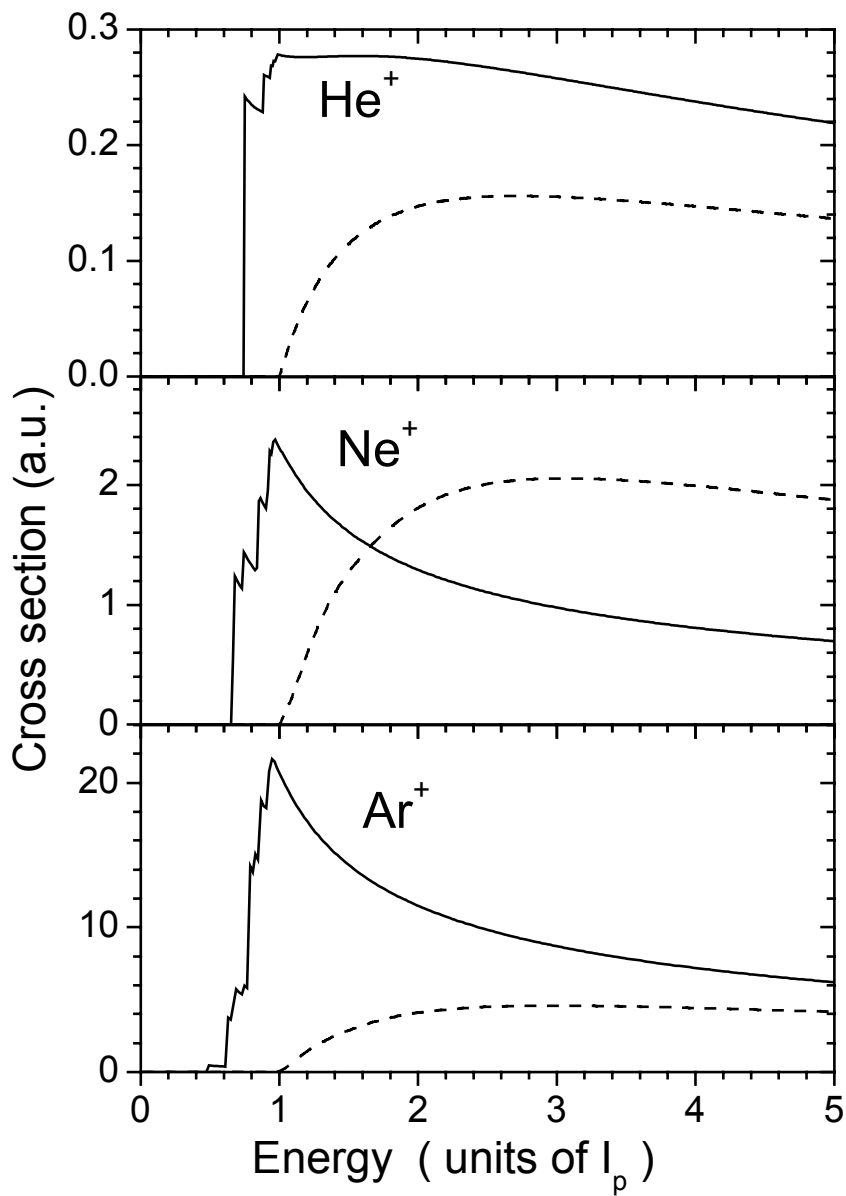


FIG. 3. Total excitation (solid lines) and ionization (dashed lines) cross sections for He^+ , Ne^+ and Ar^+ as function of the electron impact energy in units of ionization potential I_p^+ .

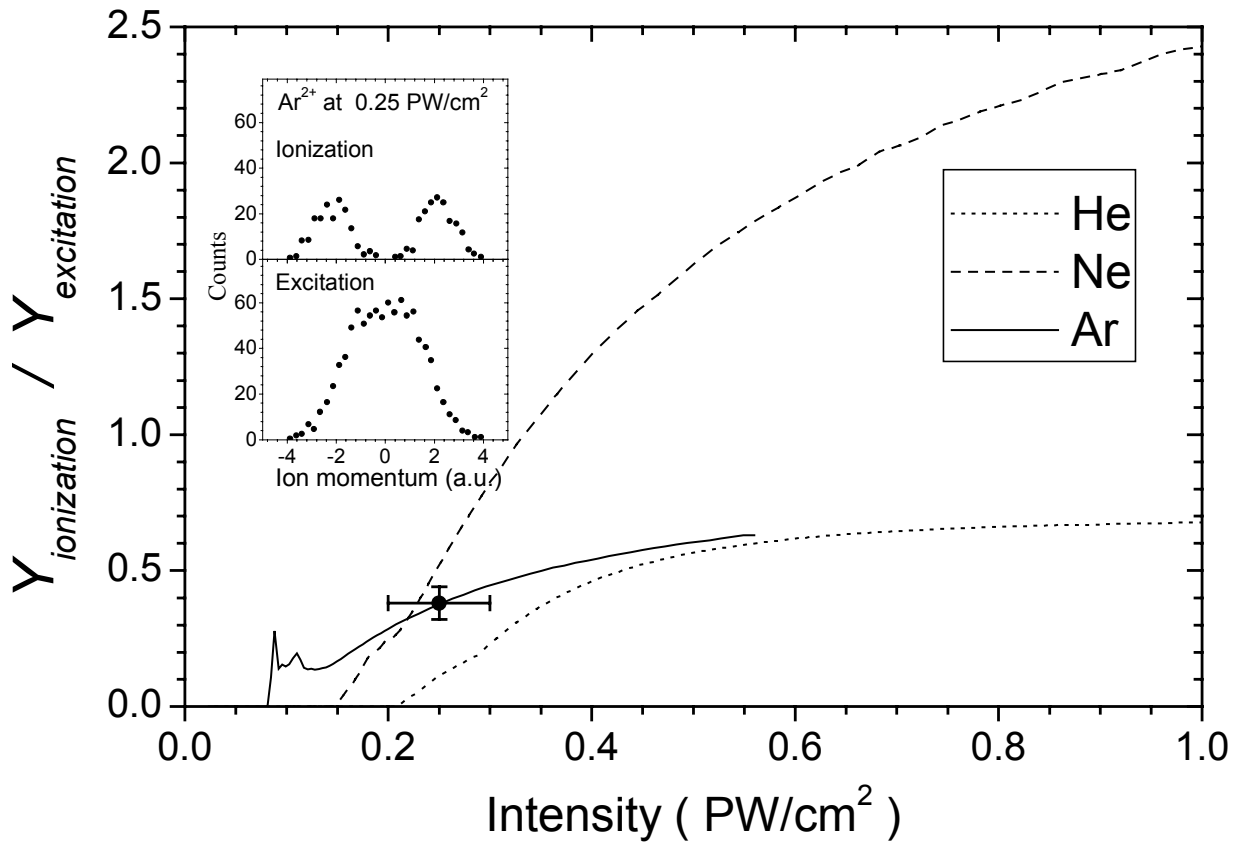


FIG. 4. Ratio of the double ionization yield for ionization and excitation according to Equation (1) based on the cross sections shown in Fig. 3 as function of the laser intensity. At 0.58 PW/cm² the suppressed I_p^+ is zero for Ar and, thus, beyond this value the calculation is not valid anymore. The experimental result for Ar from ¹⁶ $R_{exp} = 0.37(6)$ at 0.25(5) PW/cm² (the Ar²⁺ spectra are depicted on the top) is also shown in the picture.

-
- ¹ M. Protopapas, C.H. Keitel, and P.L. Knight, *Rep. Prog. Phys.* **60**, 389 (1997).
- ² R. D[^]rner, Th. Weber, M. Weckenbrock, A. Staudte, M. Hattass, H. Schmidt-B[^]cking, R. Moshhammer, and J. Ullrich, *Adv. At. Mol. and Opt. Phys.* **48**, 1 (2002).
- ³ Th. Weber, M. Weckenbrock, A. Staudte, L. Spielberger, O. Jagutzki, V. Mergel, F. Afaneh, G. Urbasch, M. Vollmer, H. Giessen, and R. D[^]rner, *Phys. Rev. Lett.* **84**, 443 (2000).
- ⁴ R. Moshhammer, B. Feuerstein, W. Schmitt, A. Dorn, C.D. Schr[^]ter, J. Ullrich, H. Rottke, C. Trump, M. Wittmann, G. Korn, K. Hoffmann, and W. Sandner, *Phys. Rev. Lett.* **84**, 447 (2000).
- ⁵ A. Becker and F.H.M. Faisal, *Phys. Rev. Lett.* **84**, 3546 (2000).
- ⁶ R. Kopold, W. Becker, H. Rottke, and W. Sandner, *Phys. Rev. Lett.* **85**, 3781 (2000).
- ⁷ M. Lein, E.K.U. Gross, and V. Engel, *Phys. Rev. Lett.* **85**, 4707 (2000).
- ⁸ J.S. Parker, L.R. Moore, K.J. Meharg, D. Dundas, and K.T. Taylor, *J. Phys. B* **33**, L691 (2001).
- ⁹ S.P. Goreslavskii, S.V. Popruzhenko, R. Kopold, and W. Becker, *Phys. Rev. A* **64**, 053402 (2001).
- ¹⁰ K. Sacha and B. Eckhardt, *Phys. Rev. A* **63**, 043414 (2001).
- ¹¹ L.B. Fu, J. Liu, and S.G. Chen, *Phys. Rev. A* **65**, 021406 (2002).
- ¹² P.B. Corkum, *Phys. Rev. Lett.* **71**, 1994 (1993).
- ¹³ B. Feuerstein, R. Moshhammer, and J. Ullrich, *J. Phys. B* **33**, L823 (2000).
- ¹⁴ H. van der Hart, *J. Phys. B* **33**, L699 (2000).

-
- ¹⁵ Th. Weber, M. Weckenbrock, A. Staudte, L. Spielberger, O. Jagutzki, V. Mergel, F. Afaneh, G. Urbasch, M. Vollmer, H. Giessen, and R. Dörmner, *J. Phys. B* **33**, L127 (2000).
- ¹⁶ B. Feuerstein, R. Moshhammer, D. Fischer, A. Dorn, C.D. Schröter, J. Deipenwisch, J.R. Crespo López-Urrutia, C. Hüller, P. Neumayer, J. Ullrich, H. Rottke, C. Trump, M. Wittmann, G. Korn and W. Sandner, *Phys. Rev. Lett.* **87**, 043003 (2001).
- ¹⁷ R. Moshhammer, J. Ullrich, B. Feuerstein, D. Fischer, A. Dorn, C.D. Schröter, J.R. Crespo López-Urrutia, C. Hüller, H. Rottke, C. Trump, M. Wittmann, G. Korn, K. Hoffmann, and W. Sandner, *J. Phys. B* **36**, L113 (2003).
- ¹⁸ J. Ullrich *et al.*, *J. Phys. B* **30**, 2917 (1997).
- ¹⁹ N. B. Delone and V. P. Krainov, *Physics - Uspekhi* **41**, 469 (1998).
- ²⁰ G. G. Paulus, W. Nicklich, Huale Xu, P. Lambropoulos, and H. Walther, *Phys. Rev. Lett.* **72**, 2851 (1994).
- ²¹ V.A. Bernshtam, Yu.V. Ralchenko, and Y. Maron, *J. Phys. B* **33**, 5025 (2000).
- ²² H.W. van der Hart and K. Burnett, *Phys. Rev. A* **62**, 013407 (2000).
- ²³ V.I. Fisher, Yu.V. Ralchenko, V.A. Bernshtam, A. Goldgirsh, Y. Maron, L.A. Vainshtein, I. Bray, H. Golten, *Phys. Rev. A* **55**, 329 (1997).
- ²⁴ D.A. Verner, E.M. Verner, and G.J. Ferland, *At. Data and Nucl. Data Tables* **64**, 1 (1996).
- ²⁵ H. van Regemorter, *Astrophys. J.* **136**, 906 (1962).